Progress In Electromagnetics Research, *PIER 31, 89–112, 2001*

ANALYSIS OF ELECTROMAGNETIC WAVE SCATTERING BY AN ELECTRICALLY LARGE METALLIC GRATING USING WAVELET-BASED ALGEBRATIC MULTIGRID PRECONDITIONED CG METHOD

R. S. Chen and D. G. Fang

Department of Electrical Engineering
Nanjing University of Science and Technology
Nanjing, 210094, China

K. F. Tsang and E. K. N. Yung

Department of Electronic Engineering
City University of Hong Kong
Kowloon, Hong Kong

Abstract–An effective wavelet based multigrid preconditioned conjugate gradient method is developed to solve electromagnetic large matrix problem for millimeter wave scattering application. By using wavelet transformation we restrict the large matrix equation to a relative smaller matrix and which can be solved rapidly. The solution is prolonged as the new improvement for the conjugate gradient (CG) method. Numerical result shows that our developed wavelet based multigrid preconditioned CG method can reach large improvement of computational complexity. Due to the automaticity of wavelet transformation, this method is potential to be a block box solver without physical background.

1. INTRODUCTION

Integral equation methods (IE) are widely used for the numerical analysis of electromagnetic radiation and scattering. However, the discretization of integral equations results in a full system of equations that, in principle, requires storage memory proportional to the square of the number of unknowns N^2 and an operation count in the direct solution proportional to N^3. Although the speed of computers has grown by leaps and bounds in the past decades, there will be a stage when the algorithms utilized to solve many engineering problems are more important than the hardware itself. The requirement for more efficient ways of analyzing electrically large structures results in a large number of recent publication [1–5]. On the other hand, most of these efficient techniques are commonly based on an iterative solution of the system of equations with Krylov subspace methods, where the matrix-vector products are optimized in one of the following two ways. (1) Exploiting the physical or mathematical properties of the matrix. Examples of this technique include the fast Fourier transform, the fast multipole method (FMM), multilevel algorithms. (2) Using sets of basis and testing functions that radiate narrow beams, and thus produce impedance matrices that contain many small elements. This technique includes impedance matrix localization (IML) and wavelet expansions. Among these techniques, multilevel method takes a different approach to large problems. This method exploits the property that any solution is composed of fast and slow spatial variations, i.e., high and low frequency components. Typically, fast spatial variations are caused by local iterations in the geometry, while slow variations arise from global interactions. By using more than one level of discretization, the slow and fast modes can quickly be identified using iterative solvers at the coarse and fine levels, respectively. These components are passed back and forth between the levels until the errors are reduced below a set threshold. Using this technique, accurate solutions can be obtained with far less computational efforts, because the amount of work required obtaining a solution is proportional to the degree of variation among the different scales or modes in a problem. As far as the best knowledge of authors, the banded matrix iteration (BMI) and Gauss-

Seidel scheme is widely used as smoother for multi-grid method while the conjugate gradient class of methods are rarely applied. One reason may be that the routine loses its memory of the spanned Krylov subspace information between calls when the solved components are passed back and forth between the levels.

Currently, preconditioning is known to be the critical ingredient in the success of iterative methods in solving many real-life problems. The computational efficiency is determined by the number of iteration to converge in the CG algorithm. Despite convergence to a correct solution is always guaranteed [6], CG method in some cases will spend much time due to the slow convergence speed or large number of iterations. The BiCG, a variation of the CG algorithm, can converge much faster than CG in many cases but the convergence is highly erratic [7]. To reduce the number of iterations, various preconditioning techniques have been used [8–15]. One widely used preconditioner is the incomplete LU (ILU) decomposition of the coefficient matrix and its block variants [8–10]. Another is based on the factorization of the approximated inverse of the coefficient matrix [11, 12]. However, to form these preconditioner, additional computing time is required, depending on the preconditioning algorithm. Most simple and easy way is to use a diagonal or diagonal inverse of the coefficient matrix as a preconditioner. Although these simple preconditioners can reduce the number of the iterations for complex problems, they don't result in a significant reduction of the number of iteration [13]. It is well known that the convergence speed is largely dependent on the condition number of coefficient matrix and the condition number will become poor as the unknown count increases for a linear equation system. A discretization of a partial differential or integral equation on a fine grid may lead to a huge system of equations. The analogous discretization on a coarse grid, however, may lead to a small system that is easy to solve [16, 17]. If a method can be found to transfer solutions on the coarse grid to the fine grid and back again, e.g., by interpolation. Typically a preconditioner of this kind does a good job of handling the low frequency components of the original problem, leaving the high frequencies to be treated by the Krylov subspace iteration in the finest grid. When this technique is iterated, it results in a sequence of coarser and coarser grids, and the multigrid iteration preconditioning technique is obtained.

In this paper, we present an effective wavelet based multi-grid pre-

conditioning technique to solve electromagnetic large matrix problem. By use of the multigrid preconditioning technique, low frequency error can be readily corrected on coarser grid. As a result, this preconditioned CG method is more efficient than the traditional one. However, the transformation matrix for classical multigrid method is mainly based on the geometric structure so that it does not easily develop a black box solver, which can be used for all the cases. By using wavelet transformation the large matrix equation is transformed to a relative smaller matrix and which can be solved rapidly [18–20]. The solution is prolonged as the initial guess for the conjugate gradient (CG) method. Numerical results show that our developed wavelet based preconditioned CG method can result in large convergence improvement for CG iterative solver. Due to the automaticity of wavelet transformation, this approach is potential to be a block box solver without physical background.

2. THEORY

2.1 Wavelets and Multiresolution Analysis

In this section, we shall briefly summarize the essentials of the wavelets and the multi-resolution analysis. The construction of the wavelets can start from a multi-resolution analysis. A sequence of closed subspaces V_m of $L^2(R)$ that satisfies the following properties is said to be a multi-resolution analysis [21–23]:

$$\forall j \in Z, \quad V_{j-1} \subset V_j \tag{1}$$

$$\bigcap_{j \in Z} V_j = \{0\} \tag{2}$$

$$\bigcup_{j \in Z} V_j = L^2(R) \tag{3}$$

$$\forall f \in L^2(R), \quad \forall j \in Z, \quad f(x) \in V_j \Leftrightarrow f(2x) \in V_{j+1} \tag{4}$$

$$\forall f \in L^2(R), \quad \forall j, n \in Z, \quad f(x) \in V_j \Leftrightarrow f(x - 2^{-j}n) \in V_j \tag{5}$$

Where $\forall$ denotes "for all", Z denotes the set of integers. Properties (1)–(3) state that $\{V_j\}_{j \in Z}$ is a nested sequence of subspaces that effectively covers $L^2(R)$, which are called the scaling space. That is, every square integrable function can be approximated as closely as desired by a function that belongs to at least one of the subspaces V_j. Property (5) states that the subspaces can be derived from one another through dilation by integer powers of 2. It also conveys an intuitive interpretation of the properties of the sequence $\{V_j\}_{j \in Z}$: The

dilated function $f(2x)$ possesses details finer than those of $f(x)$ and thus belongs to the next subspace in the resolution hierarchy. It has been shown that there exists a unique function $\ddot{o} \in L^2(R)$ with a typical width of unity, referred to as the scaling function, such that $\{\ddot{o}_{jn}\}_{n\in Z} = \{2^{j/2}\ddot{o}(2^j x - n)\}_{n\in Z}$ is an orthonormal basis of V_j. Since typical width of $\{\ddot{o}_{jn}\}_{n\in Z}$ is 2^{-j}, V_j is the space of all square integrable functions possessing details whose length scales are no more than 2^{-j}. The number 2^{-j} is therefore referred to as the resolution associated with V_j. The approximation of a function $f(x) \in L^2(R)$ at the resolution 2^{-j} can be defined as the orthogonal projection of $f(x)$ onto V_j and thus given by

$$P_j f(x) = \sum_n \ddot{o}_{jn}(x)\langle \ddot{o}_{jn}, f\rangle = \sum_n c_n^j \ddot{o}_{jn}(x) \tag{6}$$

Where $\langle , \rangle$ denotes the standard inner product in $L^2(R)$. Since $\{\ddot{o}_{jn}\}_{n\in Z}$ is not a basis for $L^2(R)$, some information is being lost in the projection described in (6). This lost information can be interpreted as the details in $f(x)$ that are finer in resolution than 2^{-j}. Due to $V_{j-1} \subset V_j$, each space V_j can be decomposed into

$$V_j = V_{j-1} \oplus W_{j-1} \tag{7}$$

Where W_{j-1} is the orthogonal complement of V_{j-1} in V_j called wavelet space. From (7) we see that

$$P_j f(x) = P_{j-1} f(x) + Q_{j-1} f(x) \tag{8}$$

Where Q_{j-1} is the orthogonal projection of W_{j-1}. This relation indicates that an approximation at a resolution 2^{-j} can be decomposed into an approximation at a lower resolution $2^{-(j-1)}$ plus the details at the resolution of 2^{-j} which are given by $Q_{j-1}f(x)$.

It can be shown [21], that for any multi-resolution approximation, there exists a function $\psi(x)$, the wavelet, such that $\{\psi_{jn}\}_{n\in Z} = \{2^{j/2}\psi(2^j x - n)\}_{n\in Z}$ is an orthonormal basis of W_j at resolution 2^{-j}. As a consequence of (7) and of property (3) of the multi-resolution analysis, we have that

$$L^2(R) = \underset{j\in Z}{\oplus} W_j \tag{9}$$

And all the spaces W_j are mutually orthogonal. This implies that when the resolution index varies from $-\infty$ to $+\infty$, the family of functions $\{\psi_{jn}(x)\}_{n\in Z}$ is an orthonormal basis of $L^2(R)$. If we express

the projections $P_{j-1}f(x)$ and $Q_{j-1}f(x)$ in Eq. (8) with an orthogonal basis for each space, we obtain

$$P_{j-1}f(x) = \sum_k c_k^{j-1}\phi_{(j-1)k}(x) \tag{10}$$

$$Q_{j-1}f(x) = \sum_k d_k^{j-1}\psi_{(j-1)k}(x) \tag{11}$$

This decomposition procedure is called the wavelet transform, where

$$c_k^{j-1} = \sum_n c_n^j \langle \phi_{(j-1)k}, \phi_{jn} \rangle \tag{12}$$

$$d_k^{j-1} = \sum_n d_n^j \langle \psi_{(j-1)k}, \psi_{jn} \rangle \tag{13}$$

Define $\mathbf{c}^j = \left\{ c_k^j, k \in Z \right\}$ and $\mathbf{d}^j = \left\{ d_k^j, k \in Z \right\}$, then the transform can be described by

$$\mathbf{c}^{j-1} = H\mathbf{c}^j \tag{14}$$

$$\mathbf{d}^{j-1} = G\mathbf{d}^j \tag{15}$$

Where H and G are the filter coefficients of the scaling function and the wavelet function, respectively [22]. Due to the low-pass characteristic of $\phi(x)$ and the high-pass characteristic of $\psi(x)$, we can see that $\mathbf{c}^{j-1}$ denotes the low frequency component whereas $\mathbf{d}^{j-1}$ denote the high frequency component. The wavelet inverse transform is defined by

$$c_n^j = \sum_k c_k^{j-1}\langle \phi_{jn}, \phi_{(j-1)k} \rangle + \sum_k d_k^{j-1}\langle \psi_{jn}, \psi_{(j-1)k} \rangle \tag{16}$$

Using Eqs. (8) and (9), we can describe Eq. (16) by

$$\mathbf{c}^j = H^a\mathbf{c}^{j-1} + G^a\mathbf{d}^{j-1} \tag{17}$$

Where superscript "a" denotes the adjoin operator, which corresponds to the transposition for a matrix. For 2-D case, the scaling space can be generated by the 1-D scaling space:

$$\mathbf{V}_j = V_j \oplus V_j \tag{18}$$

and the 2-D scaling function is defined by

$$\Phi_{jn}(x,y) = 2^j \Phi\left(2^j x - n_1, 2^j y - n_2\right) = \phi_{jn_1}(x)\phi_{jn_2}(y) \tag{19}$$

at which $\mathbf{V}_j$ defines a family nested subspaces in $L^2(R^2)$, The 2-D wavelet transform and the

inverse transform can be obtained similarly as the 1-D case [21]. The following decomposition from $\mathbf{V}_j$ to $\mathbf{V}_{j-1}$ is needed in this paper

$$\mathbf{C}^{j-1} = HH\mathbf{C}^j \tag{20}$$

The equations (14), (15), (17), and (20) can be calculated by the algorithm described in [23].

2.2 The Connection between Multigrid and Multiresolution Analysis

Within the multiresolution framework it is possible to do a very efficient decomposition of a function over all of the subspaces of interest. Given a function $u \in V_0$, the orthogonality of ϕ and ψ may be used to find coefficients c_{0k} such that

$$u(x) = \sum_k c_{0k}\phi(x-k) \tag{21}$$

This may be regarded as a fine grid representation of u. Further, coefficients c_{1k} and d_{1k} may be found for a coarse grid representation of u. On V_1 and W_1 of the form

$$u(x) = \sum_k c_{1k}\phi\left(\frac{x}{2} - k\right) + d_{1k}\psi\left(\frac{x}{2} - k\right) \tag{22}$$

This process may be continued if decomposing each V_j representation of u on the next coarser pair of grids V_{j+1} and W_{j+1} until the coarsest grid is reached. The efficient Pyramid algorithm for performing this decomposition of an $N = 2^M$ point sample of u over M levels requires $O(N)$ operations. For a general operator equation of the form, $Lu = f$ where L is a self-adjoint operator representing an elliptic boundary value problem. The notation can be simplified by letting

$$\phi_{jk} = \phi\left(2^{-j}x - k\right) \quad \text{and} \quad \psi_{jk} = \psi\left(2^{-j}x - k\right) \tag{23}$$

In addition, $< u, v >$ will denote the appropriate inner product for the problem. On the fine grid V_0 and the first coarse grid (V_1, W_1), the solution u may be represented as in (21) and (22). The data f also have a representation on V_0 and (V_1, W_1) with respective coefficients f_{0k}, f_{1k} and g_{1k}. The fine grid problem after using orthogonality in a standard Galerkin way has the form

$$\sum_k c_{1k} < \phi_{1j}, L\phi_{1k} > + d_{1k} < \phi_{1j}, L\psi_{1k} >= f_{1j} \ \forall j \tag{24}$$

and

$$\sum_k c_{1k} < \psi_{1j}, L\phi_{1k} > + d_{1k} < \psi_{1j}, L\psi_{1k} >= g_{1j} \ \forall j \tag{25}$$

The problem given in (24) may be regarded as the coarse grid problem for the smooth components of the solution, while (25) gives the coarse grid problem for the oscillatory components.

In classical multigrid algorithms, a solution is sought on a fine grid Ω^h with grid spacing h by using standard relaxation methods to approximate errors on the coarse grids Ω^{2h}, Ω^{4h}, $\cdots$. The details of the various multigrid cycles are not important for this discussion, except to say that vectors are transferred from coarse grids to finer grids with an interpolation operator denoted I_{2h}^h, while vectors are transferred from fine grids to coarser grids with a restriction operator denoted I_h^{2h}. The most common choice for interpolation is linear interpolation, while full weighting is one of the most commonly used restriction operators.

Classical multigrid methods apply limited relaxation to the fine grid problem (23). They deal only with the coarse grid equation for the smooth components (24). Furthermore, the second term of (24) representing oscillatory components is dropped and the matrix given by $< \phi_{1j}, L\phi_{1k} >$ is precisely the multigrid coarse grid operator $L^{2h} = I_h^{2h} L^h I_{2h}^h$. The entire coarse grid equation for the oscillatory components (25) is also dropped in multigrid. The rationale for neglecting the oscillatory components in (24) and (25)is that relaxation is an extremely effective way to isolate or eliminate them.

2.3 Formulation and Model of Multi-Level method of Lines

For the sake of illustration, we consider a plane wave incident on a 2-D frequency-selective surface integrated on a single substrate with rectangular apertures distributed periodically along any two skewed

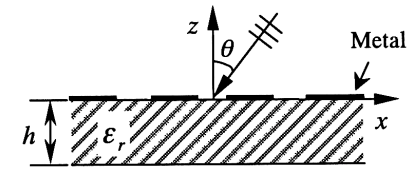

(a)

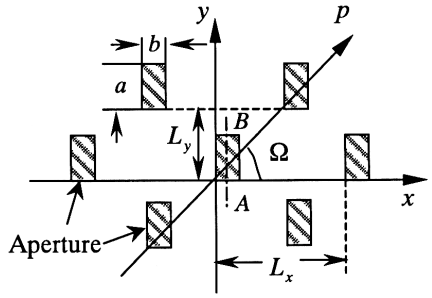

(b)

Figure 1. A 2-D frequency-selective surface integrated on a multilayered medium substrate with rectangular apertures distributed periodically along any two skewed coordinates x and p at angle Ω. (a) The side view. (b) The top view.

coordinates x and p at an angle Ω as shown in Figure 1(a). The incident angle is (θ, φ). We use Π_z^e and Π_z^h to denote the Hertz electric and magnetic potentials along z direction. Then the hybrid fields can be expressed as

$$E_x = \frac{\partial^2 \Pi_z^e}{\partial x \partial z} - j\omega\mu_0 \frac{\partial \Pi_z^h}{\partial y} \tag{26}$$

$$E_y = \frac{\partial^2 \Pi_z^e}{\partial y \partial z} + j\omega\mu_0 \frac{\partial \Pi_z^h}{\partial x} \tag{27}$$

$$H_x = \frac{\partial^2 \Pi_z^h}{\partial x \partial z} + j\omega\varepsilon_0 \frac{\partial \Pi_z^e}{\partial y} \tag{28}$$

$$H_y = \frac{\partial^2 \Pi_z^h}{\partial y \partial z} - j\omega\varepsilon_0 \frac{\partial \Pi_z^e}{\partial x} \tag{29}$$

where Π_z^e and Π_z^h satisfy Holmholtz equation and the Floquet theo-

rem as follow:

$$\left(\frac{\partial^2}{\partial x^2}+\frac{\partial^2}{\partial y^2}+\frac{\partial^2}{\partial z^2}+k_0^2\right)\Pi_z=0 \tag{30}$$

$$\Pi_z(x+L_x,y+L_y,z)=e^{-j\beta_x L_x}e^{-j\beta_y L_y}\Pi_z(x,y,z) \tag{31}$$

where $\beta_x=k_0\sin\theta\cos\varphi$, $\beta_y=k_0(\sin\theta\cos\varphi\cot\Omega+\sin\theta\sin\varphi)$, Π_z denotes Π_z^e or Π_z^h. We suppose that the Hertz potentials of incident field have the following forms

$$\Pi_z^{e,in}=c^e e^{jk_0\Theta},\quad \Pi_z^{h,in}=c^h e^{jk_0\Theta} \tag{32}$$

where $\Theta=x\sin\theta\cos\varphi+y\sin\theta\sin\varphi+z\cos\theta$. Substituting Eq. (32) into (26)–(29), we can obtain the tangential components of the incident field

$$E_x^{in}=\left(-c^e\cos\theta\cos\varphi+c^h Z_0\sin\varphi\right)e^{jk_0\Theta} \tag{33}$$

$$E_y^{in}=\left(-c^e\cos\theta\sin\varphi-c^h Z_0\cos\varphi\right)e^{jk_0\Theta} \tag{34}$$

$$H_x^{in}=\left(-c^h\cos\theta\cos\varphi-c^e Y_0\sin\varphi\right)e^{jk_0\Theta} \tag{35}$$

$$H_y^{in}=\left(-c^h\cos\theta\sin\varphi+c^e Y_0\cos\varphi\right)e^{jk_0\Theta} \tag{36}$$

where $Z_0=Y_0^{-1}=120\pi$, c^e and c^h are arbitrary constants which satisfy the relation $c^e+c^h=1$. The ratio between the constants c^e and c^h represents the proportion of TM^z mode and TE^z mode in the incident field. That means there is only TE^z incidence for $c^e=0$ and TM^z incidence for $c^h=0$. The scattering fields at point z produced by the substrate can be written by

$$\begin{aligned}H_x^s=\Big\{&-c^h T_{TM}\left(1+R_{TM}\right)\cos\theta\cos\varphi\\&-c^e Y_0 T_{TE}\left(1+R_{TE}\right)\sin\varphi\Big\}e^{jk_0\Phi}\end{aligned} \tag{37}$$

$$\begin{aligned}H_y^s=\Big\{&-c^h T_{TM}\left(1+R_{TM}\right)\cos\theta\sin\varphi\\&+c^e Y_0 T_{TE}\left(1+R_{TE}\right)\cos\varphi\Big\}e^{jk_0\Phi}\end{aligned} \tag{38}$$

where $\Phi=x\sin\theta\cos\varphi+y\sin\theta\sin\varphi-z\cos\theta$. T_{TE} and T_{TM} are the transmission coefficients from $z=0$ to z, R_{TE} and R_{TM} are the

reflecting coefficients at point z. They all can be obtained by using the wave matrix technique. By introducing the following transformation,

$$P(x,y,z) = \Pi_z(x,y,z)e^{j\beta_x x}e^{j\beta_y y} \tag{39}$$

Eq. (30) and (31) can be written as

$$\frac{\partial^2 P}{\partial x^2}+\frac{\partial^2 P}{\partial y^2}+\frac{\partial^2 P}{\partial z^2}-j2\beta_x\frac{\partial P}{\partial x}-j2\beta_y\frac{\partial P}{\partial y}+\left(k_0^2-\beta_x^2-\beta_y^2\right)P=0 \tag{40}$$

$$P(x+L_x,y+L_y,z)=P(x,y,z) \tag{41}$$

Furthermore, the boundary condition states that the tangential magnetic fields should be continuous on the aperture surfaces.

In order to solve the hybrid field problem numerically, the cell is discretised by N_x and N_y lines in the x- and y-direction with mesh widths h_x and h_y, respectively. The discretization lines for Π_z^h are shifted by $h_x/2$ and $h_y/2$ with respect to the lines for Π_z^e. Consequently, Eq. (40) can be expressed as

$$\begin{aligned}&\frac{d^2\left[P^{e,h}\right]}{dz^2}+\frac{1}{h_x^2}\left[D_{xx}\right]\left[P^{e,h}\right]+\frac{1}{h_y^2}\left[D_{yy}\right]\left[P^{e,h}\right]\\&-\frac{j2\beta_x}{h_x}\left[D_x\right]\left[P^{e,h}\right]-\frac{j2\beta_y}{h_y}\left[D_y\right]\left[P^{e,h}\right]+\left(k_0^2-\beta_x^2-\beta_y^2\right)\left[P^{e,h}\right]\end{aligned} \tag{42}$$

where $[D_{x,y}]$ and $[D_{xx,yy}]$ are the first and the second order difference matrices, respectively.

By means of the orthogonal transformation matrices $\left[T_x^{e,h}\right]$ and $\left[T_y^{e,h}\right]$, the difference matrices are transformed into diagonal matrices

$$\left[T_x^{e,h}\right]^+\left[D_{xx}\right]\left[T_x^{e,h}\right]=-\operatorname{diag}\left[d_{xxn}\right] \tag{43a}$$

$$\left[T_y^{e,h}\right]^+\left[D_{yy}\right]\left[T_y^{e,h}\right]=-\operatorname{diag}\left[d_{yyn}\right] \tag{44b}$$

and

$$\left[T_x^{e,h}\right]^+\left[D_x\right]\left[T_x^{e,h}\right]=-\operatorname{diag}\left[d_{xn}\right] \tag{45a}$$

$$\left[T_y^{e,h}\right]^+\left[D_{yy}\right]\left[T_y^{e,h}\right]=-\operatorname{diag}\left[d_{yn}\right] \tag{45b}$$

where

$$d_{xx,yy} = 4\sin^2\frac{\varphi_{x,yn}}{2}, \quad d_{x,yn} = j2e^{j\frac{\varphi_{x,yn}}{2}}\sin\frac{\varphi_{x,yn}}{2} \tag{46}$$

and

$$T^e_{x,ymn} = \frac{1}{\sqrt{N}_x}e^{jm\varphi_{x,yn}}, \quad T^h_{x,ymn} = \frac{1}{\sqrt{N}_x}e^{j(m+0.5)\varphi_{x,yn}} \tag{47}$$

with

$$\varphi_{x,yn} = \frac{2\pi(n-1)}{N_{x,y}} \tag{48}$$

So, for the elements of the transformed potential matrix

$$\left[U^{e,h}\right] = \left[T^{e,h}_x\right]^+ \left[P^{e,h}\right] \left[T^{e,h}_z\right] \tag{49}$$

one obtains the uncoupled differential equations

$$\frac{d{U^{e,h}}_{mn}}{dz^2} + k_{mn}{U^{e,h}}_{mn} = 0 \tag{50}$$

with

$$k^2_{mn} = \varepsilon_r k_0^2 - \beta_x^2 - \beta_y^2 - \frac{d_{xxm}}{h_x^2} - \frac{d_{yyn}}{h_y^2} - \frac{j2\beta_x d_{xm}}{h_x} - \frac{j2\beta_y d^*_{yn}}{h_y} \tag{51}$$
$$m = 1, 2, \cdots, N_x, \quad n = 1, 2, \cdots, N_y$$

Through the spectral domain immittance method, we can obtain the expression of current-voltage matrix equation in transformed domain.

$$\begin{bmatrix} \left[\widetilde{Z}_{xx}\right] & \left[\widetilde{Z}_{xy}\right] \\ \left[\widetilde{Z}_{yx}\right] & \left[\widetilde{Z}_{yy}\right] \end{bmatrix} \begin{bmatrix} \left[\widetilde{J}_x\right] \\ \left[\widetilde{J}_y\right] \end{bmatrix} = \begin{bmatrix} \left[\widetilde{E}^s_x\right] \\ \left[\widetilde{E}^s_y\right] \end{bmatrix} \tag{52}$$

in which $\left[\widetilde{Z}_{mn}\right]$ $(m, n = x, y)$ are diagonal matrices if the transformed quantities $\widetilde{E}_x$, $\widetilde{E}_y$, $\widetilde{J}_x$ and $\widetilde{J}_y$ are written in vector notation.

Because the final boundary condition cannot be applied in the transformed domain, equation (52) has to be transformed back into the original domain. For our case the metallic stip makes up the smaller part of the interface, so the reverse transformation is performed only

for the (reduced) number of lines that pass through the strip. Using the transformation relationship about fields and currents as follow:

$$\left\{\widetilde{E}_x\right\} = \left[T_x^h\right][E_x]\left[T_y^e\right]^* \tag{53a}$$

$$\left\{\widetilde{E}_y\right\} = \left[T_x^e\right]^+[E_y]\left[T_y^h\right]^* \tag{53b}$$

$$\left\{\widetilde{J}_x\right\} = \left[T_x^h\right][J_x]\left[T_y^e\right]^* \tag{54c}$$

$$\left\{\widetilde{J}_y\right\} = \left[T_x^e\right]^+[J_y]\left[T_y^h\right]^* \tag{54d}$$

One obtains:

$$[E_x] = \left[T_x^h\right]\left[\widetilde{E}_x\right]\left[T_y^e\right]^t \tag{55a}$$

$$[E_y] = \left[T_x^e\right]\left[\widetilde{E}_y\right]\left[T_y^h\right]^t \tag{55b}$$

with elements as

$$E_{xmn} = \sum_{k=1}^{N_x}\sum_{l=1}^{N_y} T_{xmk}^h \widetilde{E}_{xkl} T_{ynl}^e \tag{56a}$$

$$E_{ymn} = \sum_{k=1}^{N_x}\sum_{l=1}^{N_y} T_{xmk}^e \widetilde{E}_{ykl} T_{ynl}^h \tag{56b}$$

Substituting equation (52) into (56) obtains:

$$E_{xmn} = \sum_{k=1}^{N_x}\sum_{l=1}^{N_y} T_{xmk}^h T_{ynl}^e \widetilde{Z}_{xx}^{kl}\widetilde{J}_{xkl} + \sum_{k=1}^{N_x}\sum_{l=1}^{N_y} T_{xmk}^h T_{ynl}^e \widetilde{Z}_{xy}^{kl}\widetilde{J}_{ykl} \tag{57a}$$

$$E_{ymn} = \sum_{k=1}^{N_x}\sum_{l=1}^{N_y} T_{xmk}^h T_{ynl}^e \widetilde{Z}_{yx}^{kl}\widetilde{J}_{xkl} + \sum_{k=1}^{N_x}\sum_{l=1}^{N_y} T_{xmk}^h T_{ynl}^e \widetilde{Z}_{yy}^{kl}\widetilde{J}_{ykl} \tag{57b}$$

Substituting equation (54) into (57) obtains:

$$E_{xmn} = \sum_{s,t}(Z_{xx})_{mn}^{st} J_{xst} + \sum_{s,t}(Z_{x,y})_{mn}^{st} J_y^{st} \tag{58a}$$

$$E_{ymn} = \sum_{s,t}(Z_{yx})_{mn}^{st} J_{xst} + \sum_{s,t}(Z_{yy})_{mn}^{st} J_y^{st} \tag{58b}$$

with

$$(Z_{xx})^{st}_{mn} = \sum_{k=1}^{N_x}\sum_{l=1}^{N_y} T^{h}_{xmk}T^{e}_{ynl}T^{h*}_{xsk}T^{e*}_{ytl}\widetilde{Z}^{kl}_{xx} \tag{59a}$$

$$(Z_{xy})^{st}_{mn} = \sum_{k=1}^{N_x}\sum_{l=1}^{N_y} T^{h}_{xmk}T^{e}_{ynl}T^{e*}_{xsk}T^{h*}_{ytl}\widetilde{Z}^{kl}_{xy} \tag{59b}$$

$$(Z_{yx})^{st}_{mn} = \sum_{k=1}^{N_x}\sum_{l=1}^{N_y} T^{e}_{xmk}T^{h}_{ynl}T^{h*}_{xsk}T^{e*}_{ytl}\widetilde{Z}^{kl}_{yx} \tag{59c}$$

$$(Z_{yy})^{st}_{mn} = \sum_{k=1}^{N_x}\sum_{l=1}^{N_y} T^{e}_{xmk}T^{h}_{ynl}T^{e*}_{xsk}T^{h*}_{ytl}\widetilde{Z}^{kl}_{yy} \tag{59d}$$

Finally, we have the reduced equation on the metallic surfaces

$$\begin{bmatrix} [Z_{xx}] & [Z_{xy}] \\ [Z_{yx}] & [Z_{yy}] \end{bmatrix}_{\text{red}} \begin{bmatrix} [J_x] \\ [J_y] \end{bmatrix} = - \begin{bmatrix} [E^s_x] \\ [E^s_y] \end{bmatrix} \tag{60}$$

where

$$(Z_{xx})^{st}_{mn} = \frac{1}{N_xN_y}\sum_{k=1}^{N_x}\sum_{l=1}^{N_y} \widetilde{Z}^{kl}_{xx}e^{j(m-s)\varphi_{xk}}e^{-j(n-t)\varphi_{yl}} \tag{61a}$$

$$(Z_{xy})^{st}_{mn} = \frac{1}{N_xN_y}\sum_{k=1}^{N_x}\sum_{l=1}^{N_y} \widetilde{Z}^{kl}_{xy}e^{j(m-s+0.5)\varphi_{xk}}e^{-j(n-t-0.5)\varphi_{yl}} \tag{61b}$$

$$(Z_{yx})^{st}_{mn} = \frac{1}{N_xN_y}\sum_{k=1}^{N_x}\sum_{l=1}^{N_y} \widetilde{Z}^{kl}_{yx}e^{j(m-s-0.5)\varphi_{xk}}e^{-j(n-t+0.5)\varphi_{yl}} \tag{61c}$$

$$(Z_{yy})^{st}_{mn} = \frac{1}{N_xN_y}\sum_{k=1}^{N_x}\sum_{l=1}^{N_y} \widetilde{Z}^{kl}_{yy}e^{j(m-s)\varphi_{xk}}e^{-j(n-t)\varphi_{yl}} \tag{61d}$$

where $\varphi_{xk} = 2\pi(k-1)/N_x$, $\varphi_{yl} = 2\pi(l-1)/N_y$, $\widetilde{Z}$ represents the spectral Green's function, which can be obtained readily by using the spectral domain immittance method. Due to the fact that the expression (47)–(49) has the form of discrete Fourier transform, we can fill the matrix elements by using the fast Fourier transform (FFT) method. After the current distribution on the strip is determined from

Eq. (60), the scattering characteristics can be calculated in a straightforward manner. Although the structure given in Figure 1 is a periodic rectangular aperture, the above procedures are also applicable for other structures such as arbitrarily shaped aperture or screen on multi-layered microstrip circuits.

If the operator equation is then solved by LU decomposition (Gaussian elimination) or alternatively by an iterative technique such as CG method, the computational labor may be excessive for a large matrix dimension. LU decomposition requires $O(N^3)$ operations and $O(N^2)$ memory storage. CGM requires $O(N^2)$ operations per iteration and $O(N^2)$ memory storage for a dense matrix, because the most costly step in the CG method iteration is in the matrix-vector multiplication. In general, the number of iterations increases with the electrical size. The high computational complexity of the CGM precludes its application to analyze large structure problem. The idea of matrix dimension-descent technique has been employed in [16, 17], which can be expressed as:

$$R \cdot Z \cdot R^H \cdot R \cdot J = R \cdot E \tag{62}$$

But as we mentioned above, these techniques are based on the geometric basis transformation. This drawback limits its application for more complex structure in which the geometric basis transformation matrix R can not be found easily. The wavelet transformation provides us an automatic transformation, which allow us to transform an $N \times N$ matrix into an $N/2 \times N/2$ matrix without physical background. The use of multi-grid iteration preconditioning technique can speed up convergence of CG algorithm. For the complex coefficient linear equations, the preconditioned conjugate gradient method is an effective means to solve. Given an initial guess x_0, we generate a sequence x_k of approximations to the solution x as follows:

$$r_0 = b - Zx_0 \tag{63}$$

Solve $M\widetilde{r}_0 = r_0$ and $MR_0 = \widetilde{r}_0$, set $P_0 = \dfrac{R_0}{(R_0, Z^H\widetilde{r}_0)}$

For $k = 0$ step 1 until convergence do

$$M\widetilde{p}_k = Zp_k \tag{64}$$

$$\alpha_k = 1/\left(\widetilde{p}_k, Zp_k\right) \tag{65}$$

$$x_{k+1} = x_k + \alpha_k p_k \tag{66}$$

$$\widetilde{r}_{k+1} = \widetilde{r}_k - \alpha_k \widetilde{p}_k \tag{67}$$

$$\text{Solve } M\widetilde{R}_{k+1} = Z^H \widetilde{r}_{k+1}. \tag{68}$$

$$\beta_k = 1/\left(Z^H \widetilde{r}_{k+1}, \widetilde{R}_{k+1}\right) \tag{69}$$

$$p_{k+1} = p_k + \beta_k \widetilde{R}_{k+1} \tag{70}$$

Where Z^H is a transpose complex conjugate of matrix Z. The above PCG algorithm is different from the algorithm presented in [8], where the preconditioning is carried out directly to improve the condition number of linear equation system while the implementation of CG algorithm is adopted straightforward. This straightforward implementation is named explicit preconditioning and suitable for the case when preconditioning matrix M can be explicitly expressed. However, preconditioning matrix M for the multi-grid preconditioning technique can't be derived explicitly and the preconditioning process only can be applied to CG algorithm implicitly. In the following, the multigrid preconditioning is illustrated with two-level scheme as the example.

To develop a simple two-level preconditioning method, we start with the familiar operator equation:

$$Lf = g \tag{71}$$

Where L is a linear integral operator, g is a known excitation, and the function f is to be determined. For a discretization grid h, the matrix equation $\left|Z^h\right| r^h = v^h$ is obtained, where v^h is a column vector of the known excitation coefficients and r^h is a column vector of the unknown function coefficients; the superscript h denotes fine spatial sampling. Next, assume another matrix equation, $\left|Z^H\right| r^H = v^H$, is generated, where $H = 2h$ is the support associated with a set of coarser basis and weighting functions. Here, $\left|Z^H\right|$ and $\left|Z^h\right|$ correspond to fine and coarse representations of the operator L, respectively. The same thing is true of the vector pairs v^h, v^H and r^h, r^H. We can start the multilevel process at the fine level by finding iterative solution to $\left|Z^H\right| r^H = v^H$. If we denote the solution error and the residual errors as e_k^h and rr_k^h, respectively, it follows that

$$\left|Z^h\right| e_k^h = rr_k^h \tag{72}$$

The residual error contains the slow modes that are not readily accessible to the iteration process at the fine level of discretization. To continue the solution process at a coarser level, let us assume that there exist a pair of operator, $|R|$ and $|I|$, that project the residual error from the fine space to the coarse space, and vice versa. Using the restriction operator R, we project rr_k^h to the coarse level, H, and denote it rr^H, yielding

$$rr^H = |R| rr^h \tag{73}$$

where the subscript k is temporarily omitted for clarity.

The restriction operator is of the form with Daubechies order-4 wavelets

$$\mathbf{R} = \begin{bmatrix} h_0 & h_1 & h_2 & h_3 & 0 & 0 & \dots & & \dots & 0 & 0 \\ 0 & 0 & h_0 & h_1 & h_2 & h_3 & \dots & & \dots & 0 & 0 \\ 0 & 0 & 0 & 0 & h_0 & h_1 & \dots & & \dots & 0 & 0 \\ \vdots & & \vdots & & \vdots & & \dots & & \dots & \vdots & \vdots \\ 0 & 0 & \dots & & \dots & 0 & 0 & h_0 & h_1 & h_2 & h_3 \\ h_2 & h_3 & \dots & & \dots & 0 & 0 & 0 & 0 & h_0 & h_1 \end{bmatrix}_{\frac{N}{2} \times N} \tag{74}$$

And the interpolation operator $\mathbf{I}$ is related to $\mathbf{R}$ through transposition. Since $H > h$, the low frequency (i.e., slow) components of rr^h are transformed to high frequency (i.e., fast) components in rr^H. The solution at this level can be found by LU factorization if the number of unknowns is small enough, or by iteration if number of unknowns N is still relatively large. Once obtained, the coarse version of the error e^H is projected to the fine level via the interpolation operator, $|I|$. The result is an improved value of e^h, which we denote by $\widetilde{e}^h$:

$$\widetilde{e}^h = |I| e^H \tag{75}$$

A new estimate of the solution is then available by adding $\widetilde{e}^h$ to the previous estimate of the solution at the fine level and then the preconditioning process in equation (7) in the above CG algorithm is completed.

$$\widetilde{r}_k^{\text{new}} = r_k^{\text{old}} + \widetilde{e}^h \tag{76}$$

where the "old" and "new" superscripts signify the estimates of the solution before and after the coarse level correction. The new estimate contains slow-mode information not easily obtained at the fine

level. It also contains fast mode errors introduced by the interpolation process (14). These fast mode errors, however, can be removed in a few iterations at the fine level. The iterative procedure at the fine level again is halted when the convergence starts to stall and the residual error is projected down for another coarse level correction. The two-level scheme allows us to understand the basic nature of multilevel method. In practice, however, the number of levels employed is usually more than 2. Ideally, one wants to have as many levels, as possible, so that the cost of factorization at the coarsest level is negligible. In these cases, iterations are performed on a number of levels, where the residual error at the upper levels is projected down to the lower levels using the restriction operators. Since the slow modes on a fine level seem fast on a coarser level, the iterative solver at each successive level is able to extract some of these modes, and pass the ones that are not accessible down to coarser levels. The wavelet transformation provides us an automatic transformation, which allow us to transform a $N \times N$ matrix into a $N/2 \times N/2$ matrix without physical background [18–20]. According to equation (31), we can construct the L level preconditioning process as follows: (1) using the 2-D wavelet transformation to get a dimension-descent matrix Z^{l-1}, which can be described as $Z^{l-1} = R \cdot Z^l \cdot R^H$, and repeat the transformation until the matrix dimension is small enough. (2) Using the 1-D wavelet transformation to get a dimension-descent vector E^{l-1}, which can be expressed as $E^{l-1} = R \cdot E^l$. (3) Solving a dimension-descent matrix equation by using iterative method or Gausian elimination method, due to the small dimension this procedure needs less CPU time. (4) Using the 1-D wavelet inverse transformation to get the prolongation solution E, which can be described as $E^l = R^H \cdot E^{l-1}$, and several smoothing iterations are done using CG to reduce the transformation error.

3. RESULTS AND DISCUSSIONS

To confirm the validity of our method, A numerical testing is performed by use of analyzing a frequency-selective surface. The structure has a conducting screen perforated periodically by rectangular apertures integrated on a single substrate as shown in Figure 1. The parameters are used as follows: $\Omega = 18.4°$, $\varepsilon_r = 2.22$, $h = 0.254\,\text{mm}$, $L_x = 14.5\,\text{mm}$, $L_y = 1.45\,\text{mm}$, $a \times b = 3.3 \times 0.3\,\text{mm}$, $\theta = 45°$, $\varphi = 0°$. The excitation is a TE normal incidence. After discretization by the MOL

described in the section above, we obtain an operator equation like (60), which is solved iteratively by using the wavelet-based multigrid preconditioned CG method. Let u_l, u_l^0 and u_l^γ be the exact solution, the initial value of iteration, and the intermediate solution after γ-steps of iteration, respectively. The error is defined as $v_l^\gamma = u_l^\gamma - u_l$. Figure 2 shows the initial error, the 1-step and the 2-step iterative errors of the real and the imaginary part of the surface current on the aperture at A-B cut as well as the results of the wavelet transform. From the curves in Figure 2 (a1) and (a2) we can see that the error is smoothed out with the increase in the number of iterative steps. In other words, the high frequency components of the error are suppressed effectively. Now we transform these errors by using the wavelet decomposition algorithm. The Daubechies wavelet [21] is employed. The errors serve as the expansion coefficients $\mathbf{c}^l$ of the scaling function in the finest resolution space V_l. Fig. 2 (b1) and (b2) show the expansion coefficients $\mathbf{d}^{l-1}$ in the coarser level wavelet space W_{l-1}, Figure 2 (c1) and (c2) give $\mathbf{c}^{l-1}$ in the coarser level scaling space V_{l-1}. It is observed that the coefficients in the wavelet space reduce sharply after 1-step iteration as evident from Figure 2 (b1) and (b2), and they are very small after 2-step iteration. Figure 2 (c1) and (c2) show that the errors keep their profiles in the scaling space. Therefore we may come to the conclusion that the high frequency error components correspond to the ones in the wavelet space and the smooth components correspond to the ones in the scaling space. According to the above analysis, we may consider the scaling spaces as the coarse level in the multi-level MOL and thus the wavelet-based multi-level MOL is developed. In this paper, the Daubechies wavelet with 4-order vanishing moment [21] is used. The simulation and experimental results are shown in Figure 3 and they are observed in good agreement. In order to test the efficiency of our proposed wavelet based multigrid-preconditioned CG algorithm, the convergence behaviors of PCG with two-level multigrid matrix as preconditioner are tested. The computer time versus the dimension is given in Fig. 4. It can be observed that the multigrid preconditioned CG method needs smaller CPU time (PIII 500) than the direct CG one to reach $-70\,\mathrm{dB}$ residual errors.

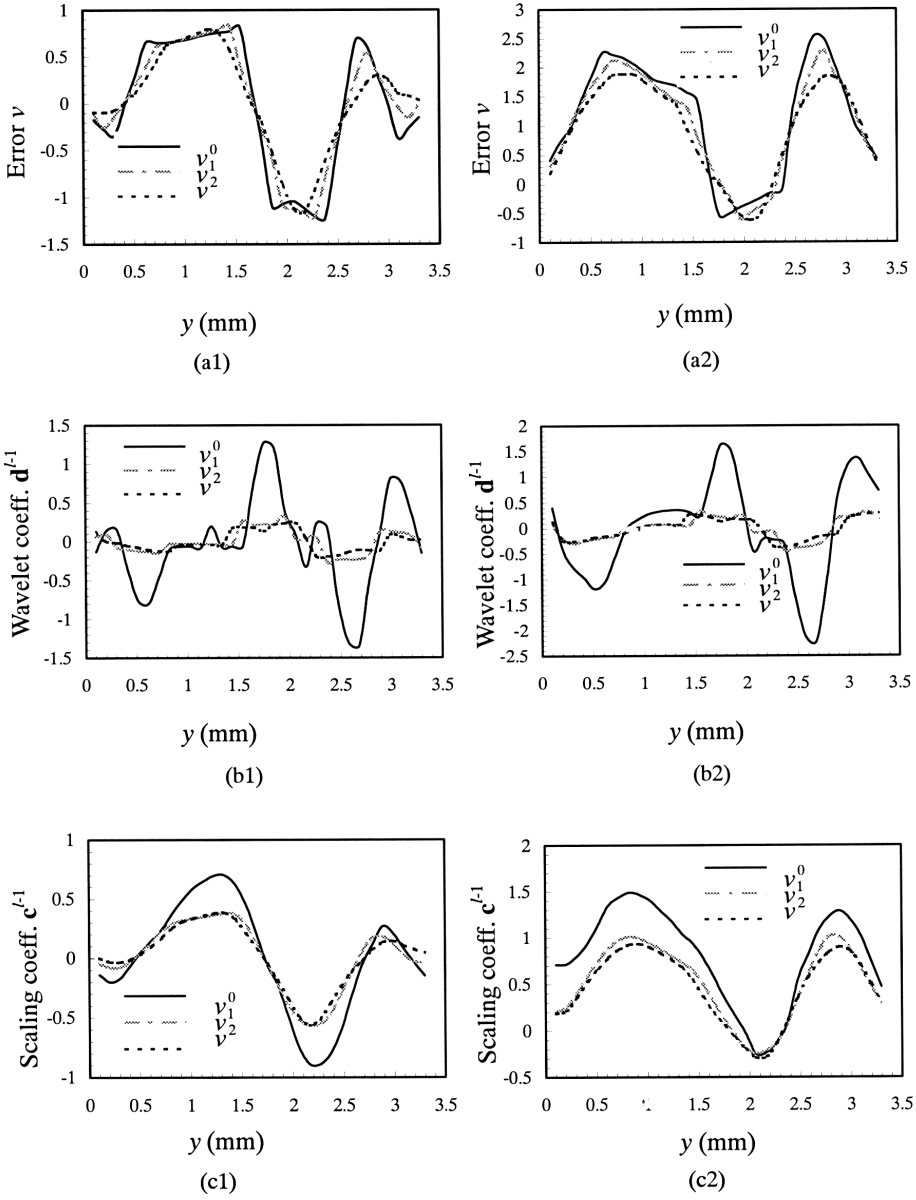

Figure 2. The iterative error of surface magnetic current M_y on the surface of the aperture and their wavelet transform coefficients in coarser level. (a1) and (a2), (b1) and (b2), (c1) and (c2) denote the real part and imaginary part of the error, wavelet coefficient, scaling coefficient, respectively.

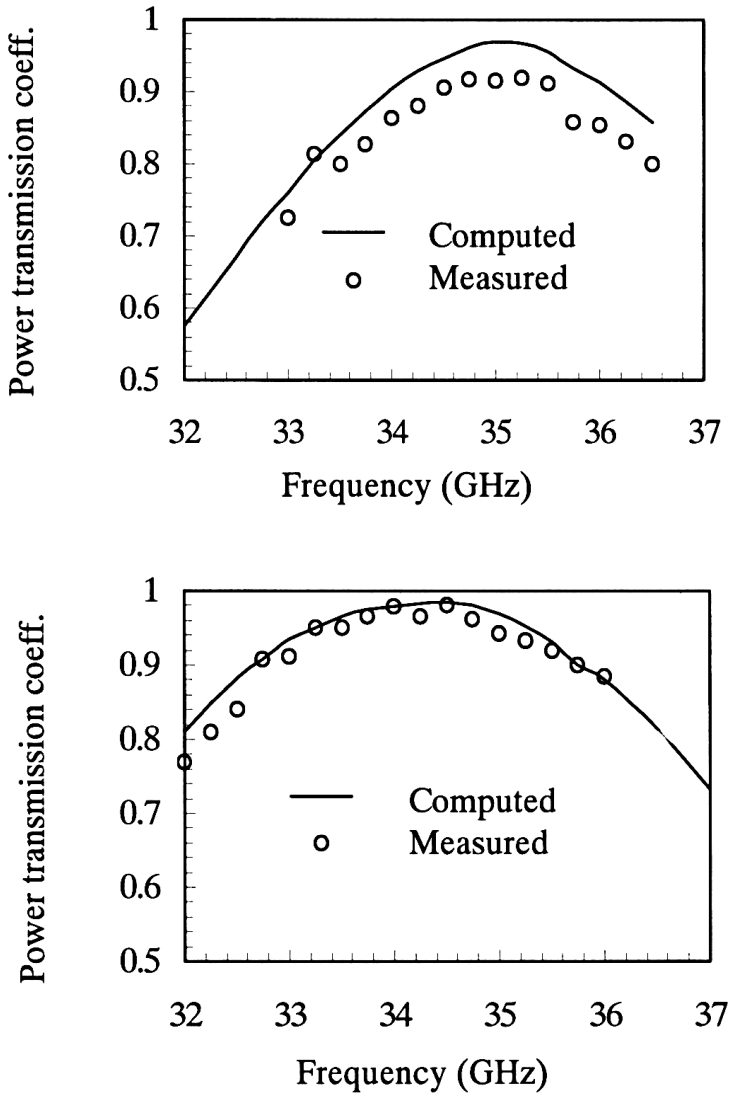

Figure 3. Power transmission coefficient of a frequency-selective surface with a conducting screen perforated periodically rectangular apertures integrated on a single substrate as shown in Fig. 1 the parameters of the structure are the same as those in IV A. (a) TE incident wave. (b) TM incident wave.

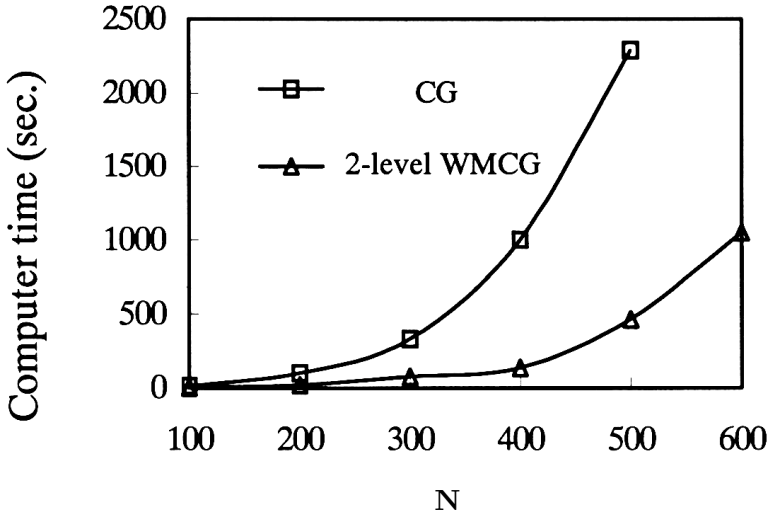

Figure 4. The computer time for different methods versus matrix dimension N.

4. CONCLUSIONS

In this paper, a new fast multigrid preconditioned CG algorithm is presented. With arbitrary oblique incidence, a new Helmholz equation as well as boundary condition is utilized to calculate the elements of impedance matrix of current-voltage reduced linear equations. Then, an effective implicit multigrid preconditioned CG algorithm is developed to solve reduced current-voltage equations. For wavelet based multigrid technique, its formulations use simple, near-orthogonal basis functions that still allow for an orthogonal decomposition of the fine grid space and similar decompositions of subsequent coarse grid spaces. Furthermore, it does not attempt to solve for the oscillatory components of the solution directly, but rather lets relaxation handle them indirectly. This choice of departing from orthogonality and incorporating relaxation as well as the residual equation accounts for the extreme efficiency of wavelet based multigrid CG algorithms. Numerical result shows that with linear coefficient matrix in coarse grid as the preconditioner, PCG algorithm can converge much faster than the conventional CG one.

REFERENCES

1. Coifman, R., V. Rohklin, and S. Wandzura, "The fast multipole method for the wave equation: A pedestrian description," *IEEE Antennas Propagat Mag.,* Vol. 35, 7–12, 1993.
2. Song, J., C. C. Lu, and W. C. Chew, "Multilevel fast multipole algorithm for electromagnetic scattering by large complex objects," *IEEE Trans Antennas Propagat.,* Vol. 45, 1488–1493, 1997.
3. Michelsen, E. and A. Boag, "A multilevel matrix decomposition algorithm for analyzing scattering from large structures," *IEEE Trans Antennas Propagat.,* Vol. 44, 1086–1093, 1996.
4. Canning, F. X., "Improved impedance matrix localization method," *IEEE Trans Antennas Propagat.,* Vol. 41, 659–667, 1993.
5. Song, J. M., C. C. Lu, W. C. Chew, and S. W. Lee, "Fast Illinois solver code (FISC)," *IEEE Antennas Propagat Mag.,* Vol. 40, 27–34, 1998.
6. Sarkar, T. K. and E. Arvas, "On a class of finite step iterative methods (conjugate directions) for the solution of an operator equation arising in electromagnetics," *IEEE Trans. Antennas and Propagat.,* Vol. 33, No. 10, 1058–1066, Oct. 1985.
7. Saad, Y., "Iterative methods for sparse linear systems," PWS Publishing Company, Boston, 1995.
8. Chen, R. S., E. K. N. Yung, C. H. Chan, and D. G. Fang, "Application of preconditioned CG-FFT technique to method of lines for analysis of the infinite-plane metallic grating," *Microwave and Optical Technology Letters,* Vol. 24, No. 3, 170–175, Feb. 5, 2000.
9. Axelsson, O. and L. Yu. Kolotilina, "Preconditioned conjugate gradient methods," Proceedings 1989, in *Lecture Notes in Mathematics,* Vol. 1457, Edited by A. Dold, B. Eckmann, and F. Takens, Springer-Verlag 1990.
10. Kershaw, D. S., "The incomplete Cholesky-conjugate gradient method for the solution of systems of linear equations," *J. Comput. Phys.,* Vol. 26, 43–65, 1978.
11. Dupont, T., R. P. Kendall, and H. H. Rachford, "An approximate factorization procedure for solving self-adjoint elliptic difference equations," *SIAM J., Numer. Anal.,* Vol. 5, No. 3, 559–573, 1968.
12. Ahn, C. H., W. C. Chew, J. S. Zhao, and E. Michielssen, "Numerical study of approximate inverse preconditioner for two-dimensional engine inlet problems," Electromagnetics, *Journal of Electromagn. Waves Appl.,* Vol. 19, No. 1, 131–146, 1999.
13. Canning, F. X., "Diagonal preconditioners for the EFIE using a wavelet basis," *IEEE Trans. Antennas Propagat.,* Vol. 44, 1239–1246, 1996.

14. Yaghjian, A. D., "Banded matrix preconditioning for electric-field integral equations," *IEEE APS Int. Symp. Dig.,* 1806–1809, Montreal, Canada, 1997.
15. Tsang, L., C. H. Chan, H. Sangani, A. Ishimaru, and P. Phu, "A banded matrix iterative approach to monte carlo simulations of large-scale random rough-surface scattering," *Journal of Electromagn. Waves Appl.,* Vol. 7 No. 9, 1185–1200, 1993.
16. Wei, C., N. Inagaki, and W. Di, "Dimension-descent technique for electromagnetic problems," *IEE Proc. Microw. Antennas Propag.,* Vol. 144, No. 5, 372–376, Oct. 1997.
17. Ooms, S. and D. De Zutter, "A new iterative diakoptic-based multilevel moments method for planar circuits," *IEEE Trans. Microw. Theory and Tech.,* Vol. 46, No. 3, 280–291, Mar. 1998.
18. Briggs, W. L. and V. E. Henson, "Wavelets and multigrid," *SIAM J. Sci. Comput.,* Vol. 14, No. 2, 506–510, March 1993.
19. Xiang, Z. and Y. Lu, "An effective wavelet matrix transform approach for efficient solutions of electromagnetic integral equations," *IEEE Trans. Antennas Propagat.,* Vol. 45, 1205–1213, 1997.
20. Wang, G., R. W. Dutton, and J. Hou, "A fast wavelet multigrid algorithm for solution of electromagnetic integral equations," *Microwave and Optical Technology Letters,* Vol. 24, No. 2, 86–91, Jan. 2000.
21. Mallat, S., "A theory for multi-resolution signal decomposition: the wavelet transform," *IEEE Trans. Pattern and Mech. Intel.,* Vol. 11, No. 7, 674–693, 1989.
22. Daubechies, I., "Orthonormal bases of compactly supported wavelets," *Commun. Pure and Appl. Math.,* Vol. 41, 909–996, 1988.
23. Beylkin, G., R. Coifman, and V. Rokhlin, "Fast wavelet transforms and numerical algorithms I," *Commun. Pure Appl. Math.,* Vol. 44, 141–183, 1991.
24. Uchida, K., T. Noda, and T. Matsumaga, "Spectral domain analysis of electromagnetics wave scattering by infinite plane metallic grating," *IEEE Trans. Antennas and Propagat.,* Vol. 35, No. 1, 46–52, 1987.